ISSN: 2837-4835

Research Article

International Internal Medicine Journal

Endocytosis and Transport of Silica Nanoparticles in BeWo b30 Cells

Mengyao Wu[2], Weijie Jiang[2], Junyu He[3], Hongbo Tang[1]*, Haibo He[2]*, Jihong Zhang[5] and Hongwu Wang[4]*

[1]*Department of Pharmacy, Beijing Obstetrics and Gynecology Hospital, Capital Medical University, Beijing Maternal and Child Health Care Hospital, Beijing, China*

[2]*Hubei Key Laboratory of Natural Products Research and Development, College of Biological and Pharmaceutical Sciences, China Three Gorges University, Yichang, Hubei, China*

[3]*Department of Clinical Medicine, Basic Medical College of China Three Gorges University, Yichang, Hubei, China*

[4]*Department and Institute of Infectious Disease, Tongji Hospital, Tongji Medical College, Hua Zhong University of Science and Technology, Wuhan, Hubei, China*

[5]*Hospital of Traditional Chinese Medicine & Hubei Clinical Medical Research Centre of Traditional Chinese Medicine for Functional Digestive Diseases, Three Gorges University, Yichang, Hubei, China*

***Corresponding Author**

Hongbo Tang, Department of Pharmacy, Beijing Obstetrics and Gynecology Hospital, Capital Medical University, Beijing Maternal and Child Health Care Hospital, Beijing, China.

Haibo He, Hubei Key Laboratory of Natural Products Research and Development, College of Biological and Pharmaceutical Sciences, China Three Gorges University, Yichang, Hubei, China.

Hongwu Wang, Department and Institute of Infectious Disease, Tongji Hospital, Tongji Medical College, Hua Zhong University of Science and Technology, 1095, Jie fang Avenue, Wuhan, Hubei, China.

Submitted: 2024, Jul 31; **Accepted**: 2024, Aug 16; **Published**: 2024, Aug 29

Citation: Wu, M., Jiang, W., He, J., Tang, H., He, H., et al. (2024). Endocytosis and Transport of Silica Nanoparticles in BeWo b30 Cells. *Int Internal Med J, 2*(8), 01-11.

Abstract

An understanding of the transport of silica nanoparticles (NPs) across the placental barrier is important in perinatal medicine. The cytotoxicity of silica NPs was investigated in this study. In up-take assays, we examined the size of NPs, as well as the effects of various inhibitors, on the internalization of silica NPs in BeWo b30 cells.

The expression levels of PI3K, AKT and GSK3β were assessed after the cells were treated with silica NPs and/or the PI3K/AKT signaling pathway inhibitor LY294002. The integrity of the cell monolayer was assessed by culturing cells on Transwell inserts and measuring the transepithelial electrical resistance, assessing fluorescein sodium transport, and staining the tight junction protein zonula occludens-1. Silica NPs were spherical in shape, and concentrations <300 μg/mL were not cytotoxic. The internalization of silica NPs with a diameter of 50 nm and 100 nm was greater than that of silica NPs with a diameter of 20 nm. CPZ manifested the most pronounced inhibitory effects with inhibition rates of 20-nm, 50-nm and 100-nm silica NPs reaching 57.5%, 49.6% and 46.9%, respectively, which indicated that silica NPs were internalized through clathrin- and caveolae-mediated endocytosis. Furthermore, LY294002 affected the uptake of 100-nm silica NPs dose-dependently. The treatment of cells with silica NPs also elevated the levels of p-PI3K/PI3K, p-AKT/AKT and p-GSK3β/GSK3β, while LY294002 inhibited the levels of these proteins, which manifested that the internalization of silica NPs was regulated by the PI3K/AKT/ GSK3β signaling pathway. Taken collectively, these results provided new insights on the transplacental transport of NPs in perinatal medicine.

Keywords: Endocytosis, Placental Barrier, PI3K/AKT/GSK3β Signaling Pathway, Silica Nanoparticles, Transport

In brief

Silica nanoparticles can cross the monolayer placental barrier model of BeWo b30 in vitro, and the endocytosis pathway is mainly mediated by clathrin and caveolin.

PI3K/Akt/GSK3β signaling pathway may play an important regulatory role in the uptake and transport of Silica nanoparticles.

1. Introduction

Over the past 20 years, nanotechnology has been used in the diagnosis and treatment of a variety of diseases [1]. Nanomedicine involves the use of nanoparticles (NPs), which can be used in magnetic resonance imaging, biosensor development, and drug delivery, as they facilitate targeted drug delivery and increase drug bioavailability. Nanomedicine also has great potential in the

treatment of maternal, fetal, and placental disorders. However, it is not known if NPs safe for use in pregnant women2, and therefore, it is important to investigate the transplacental transport of NPs in this population [2-4].

NPs interact with components of the extracellular matrix and the plasma membrane and enter cells through endocytosis, which is an important mechanism for the transport of NPs across the maternal-fetal barrier, and there are five different types of endocytosis, namely, caveolin-mediated endocytosis, phagocytosis, clathrin-mediated endocytosis, clathrin/caveolae-independent endocytosis, and micropino-cytosis. Macromolecules, such as NPs, typically enter the placenta by pinocytosis/endocytosis and phagocytosis. BeWo b30 cells are human placental trophoblast cells that are often used to study transplacental transport mechanisms [27]. Li and his colleagues investigated the transport of nine compounds and demonstrated a good correlation (R2 = 0.95) between the transport indices of BeWo b30 cells and ex vivo models prepared biodegradable digoxin-loaded PEG ylated poly (lactic-co-glycolic acid) NPs using a modified solvent displacement method and examined the permeability of these NPs across the BeWo b30 cell monolayer [6,28]. The results revealed that NPs exhibited sustained drug release kinetics, and nanoencapsulation could protect digoxin from P-glycoprotein (P-gp)-mediated efflux, thereby increase maternal-to-fetal drug transfer. Kloet and his fellow scientists analyzed the transport of NPs across the placental barrier using one positively-charged and two negatively-charged polystyrene NPs (PS-NPs) of similar size and revealed that the transport of PS-NPs across the BeWo b30 cell monolayer was not related to charge [7]. The specific transport mechanisms were also investigated using inhibitors of endocytosis or ATP-binding cassette transporters, and inhibitors of breast cancer resistance protein (BCRP), P-gp, clathrin, and caveolin did not affect the transport of PS-NPs. Previously, we prepared fluorescein isothiocyanate (FITC) conjugated pullulan acetate (PA-FITC) NPs and investigated transplacental transport using the BeWo b30 cell line. We found that these NPs, which were nontoxic, could cross the blood-placental barrier, and BeWo b30 cells could internalize PA-FITC NPs through caveolae-mediated endocytosis and pinocytosis [8]. Although this research area has received significant attention, there are few studies on the transport of NPs across the placental barrier.

Silica NPs have been studied for their use as drug carriers or imaging agents. Properties, such as tunable size and shape, high surface area, and large pore volume, make mesoporous silica NPs particularly advantageous for controlled drug release [9]. However, there are few studies on the use of silica NPs in pregnancy. Yamashita and his colleagues administered 70-nm, 300-nm and 1000-nm silica NPs into pregnant mice and observed that only the 70-nm particles were distributed in the placenta [10]. However, these findings might not be applicable to pregnant women due to structural and functional differences between the species [11]. An article investigated the transport of 20-nm and 50-nm silica NPs across the BeWo b30 cell monolayer and the ex vivo perfused human placenta and revealed that the transport of silica NPs was limited with an apparent permeability of 1.54 $\times 10^{-6} \pm 1.56 \times 10^{-6}$ cm/sec [12]. Furthermore, the percentage of 25-nm and 50-nm silica NPs reaching the fetal perfusate after 6 h was limited to 4.2 ± 4.9% and 4.6 ± 2.4%, respectively. The particles also accumulated both *in vitro* and *in vivo*, as confirmed by confocal microscopy. Therefore, silica NPs can cross the placental barrier, although the mechanism is unknown.

In this study, we examined the cytotoxicity of silica NPs using BeWo b30 cells. We investigated the possible mechanisms of transport and demonstrate the role of the phosphatidylinositol 3-kinase/protein kinase B/glycogen synthase kinase 3β (PI3K/AKT/GSK3β) signaling pathway in the internalization of silica NPs. The integrity of the BeWo b30 cell monolayer was also evaluated in transepithelial electrical resistance and fluorescein sodium (Na-Flu) transport assays, as well as tight junction protein staining. After determining the nontoxic concentration of silica NPs, their transport mechanism was assessed using the in vitro model.

2. Materials and Methods

2.1 Materials

Transwell (diameter, 12 mm; pore size, 3.0 μm) polycarbonate membrane inserts and 96-well opaque cell culture plates were purchased from Corning (Corning, NY, USA). The Millicell electrical resistance system was procured from Millipore (Bedford, MA, USA). The Cell Counting Kit-8 was purchased from Dojindo Laboratories (Kumamoto, Japan). Silica NPs of different sizes were procured from Suzhou Derivative Biotechnology (Suzhou, China). The BeWo b30 cell line was a gift from Professor Erik Rytting (University of Texas Medical Branch, Galveston, TX, USA).

DMEM-F12 was purchased from Hyclone Corp (Logan, UT, USA). Phenol red-free DMEM-F12 and fetal bovine serum (FBS) were purchased from Thermo Fisher Scientific (Waltham, MA, USA). The rabbit anti-human zonula occludens-1 (ZO-1) antibody and the goat anti-rabbit secondary antibody (conjugated to Alexa Fluor-488) were purchased from Thermo Fisher Scientific. Pharmacological inhibitors, Na-Flu salt, dimethyl sulfoxide and 4′,6-diamidino-2-phenylindole (DAPI) were procured from Sigma-Aldrich (St. Louis, MO, USA). Trypsin, Hank's balanced salt solution, and Triton X-100 were purchased from Beijing Solarbio Technology (Beijing, China).

Phosphorylation-specific antibodies against GSK3β (S9) and Akt (S473), as well as antibodies against GSK3β, PI3K-p85, β-actin and AKT, were procured from Cell Signaling Technology (Danvers, MA, USA). The phosphorylation-specific PI3K-p85 (Tyr458) antibody was purchased from Abcam (Cambridge, UK).

2.2 Characterization of Silica NPs

Silica NPs with diameters of 20, 50 and 100 nm were labeled with rhodamine B, diluted with water (stock concentration, 25 mg/mL), and stored at 4°C. The size distribution of the silica NPs was measured by dynamic light scattering (DLS, Malvern Instruments Ltd., Malvern, UK). The average size was determined from SEM images by averaging the diameters of

100 particles. The morphology of the silica NPs was observed by transmission electron microscopy (TEM, JEOL Ltd., Tokyo, Japan) and scanning electron microscopy (SEM, Carl Zeiss Microscopy GmbH, Jena, Germany). For TEM, a drop of the NP suspension was deposited on a copper grid and air-dried prior to observation. For SEM, a drop of the NP suspension was placed on a silicon wafer and air-dried. Subsequently, the samples were coated with gold for observation.

2.3 Cell Culture

BeWo b30 cells were cultured in DMEM-F12, containing phenol red, 10% FBS, 4 mM L-glutamine, and 1% penicillin-streptomycin at 37°C in a humidified atmosphere with 5% CO_2. Upon reaching 75-80% confluence, the cells were subcultured using a 0.25% trypsin-EDTA solution.

2.4 CCK-8 Cytotoxicity Assay

BeWo b30 cells (1×10^4 cells/well) were seeded in 96-well plates and cultured for 24 h. The cells were treated with silica NPs at different concentrations (200, 300, 400, 600, 800 µg/mL) for 24 and 48 h. Untreated cells served as the negative control.

Subsequently, the culture supernatant was removed, the cells were washed in PBS, CCK-8 reagent was added (10 µL of CCK-8 in 100 µL of medium), and the cells were incubated for 90 mins. The absorbance was measured at a wavelength of 450 nm with a microplate reader. The percentage of viable cells (CV%) was calculated as follows:

CV% = optical density (test)/optical density (control) × 100%.

2.5 Uptake of Silica NPs with Different Particle Sizes and Concentrations

BeWo b30 cells (1×10^4 cells/well) were seeded in 96-well opaque plates and cultured for 24 h, as indicated above. Subsequently, the culture supernatant was removed, silica NPs were added at different concentrations (75, 150, 300 µg/mL), and the cells were incubated for 5 h. The cells were washed three times with ice-cold PBS, and cell lysis solution (100 µL of 0.3% Triton X-100) was added for 1 h, after which the fluorescence intensity was measured, as indicated above. The cells cultured in the absence of NPs served as the blank control, and the cells cultured in the presence of NPs at the same concentration served as the negative control.

2.6 Effects of Inhibitors on the Uptake of Silica NPs

BeWo b30 cells (1×10^4 cells/well) were seeded in 96-well opaque plates, as indicated above. Subsequently, the culture supernatant was removed, silica NPs were added at a concentration of 300 µg/mL, and the cells were incubated for 5 h. The cells were washed three times with ice-cold PBS, and cell lysis solution (100 µL of 0.3% Triton X-100) was added for 1 h, after which the fluorescence intensity was measured, as indicated above. The uptake of silica NPs was expressed as the optical density. The percent uptake was calculated as follows: uptake (%) = (fluorescence intensity [test]/ fluorescence intensity [control]) × 100%.

To examine the effects of inhibitors of endocytosis on the uptake of silica NPs, the cells were pre-incubated with CPZ at 7 µg/mL to inhibit clathrin-mediated endocytosis, NY at 50 µg/mL to inhibit caveolae-mediated endocytosis, Col at 10 µg/mL to inhibit pinocytosis, and AMR at 50 µM to inhibit micropinocytosis for 1 h as previously described [8]. Subsequently, the culture supernatant was removed, silica NPs were added at a concentration of 300 µg/mL, and the cells were incubated for 5 h.

The cells were washed as indicated above. The cells cultured in the presence of silica NPs but in the absence of inhibitor served as the negative control. The uptake rate was expressed as 100%. The percent uptake was calculated as follows: uptake (%) = (fluorescence intensity [test]/fluorescence intensity [control]) × 100%.

To examine the activation of the PI3K/AKT pathway by silica NPs, the cells were pre-incubated with the PI3K/AKT inhibitor LY294002 at different concentrations (2.5, 5, 10 µM) for 30 min. Subsequently, the culture supernatant was removed, silica NPs in medium containing the inhibitor at the indicated concentrations were added, and the cells were incubated for 2 h. The percent uptake was calculated, as indicated above.

2.7 Western Blot Assay

BeWo b30 cells were incubated with LY294002, as indicated above. Subsequently, the culture supernatant was removed, silica NPs in medium containing the inhibitor at the indicated concentrations were added, and the cells were incubated for 2 h. The cells cultured in the absence of the inhibitor served as the negative control, whereas the cells cultured in the presence of silica NPs but in the absence of the inhibitor served as the positive control. The cells were terminated by cell lysis buffer (50 µL of 0.3% Triton X-100), containing phosphatase inhibitor cocktail (1:100) and phenylmethylsulfonyl fluoride (1:100). The cells were frozen and thawed three times, and the samples were centrifuged (4°C, 12000 rpm, 5 min). The protein concentration was measured by the BCA method. Subsequently, equivalent amounts of protein were separated by SDS-PAGE. The proteins were transferred to PVDF membranes, and the membranes were blocked with 5% bovine serum albumin for 2 h and incubated with primary antibodies for 18 h at 4°C. The membranes were washed with TBST three times, 10 min each time, and incubated with secondary antibodies for 70 min at room temperature. The target proteins were visualized with the Automatic Chemilumine- scence Imaging Analysis System (Shanghai Tianneng Technology Co., Ltd, China), and the relative gray-scale values were analyzed with Image Studio Software (Shanghai Tianneng Technology Co., Ltd, China).

2.8 Establishment of in Vitro Placental Model

Upon reaching 80-85% confluence, BeWo b30 cells (1×10^5 cells/insert) were seeded in Transwell inserts and cultured for 7 days, as indicated above. Transepithelial electrical resistance (TEER) was measured each day as previously described [13]. On day 6, the transport of Na-Flu was assessed, and the tight junction protein ZO-1 was stained.

2.9 Transport of Silica NPs

This experiment required the use of phenol red-free DMEM-F12. BeWo cells (1×10^5 cells/insert) were seeded on Transwell inserts and cultured for 24 h until confluence.

Subsequently, the culture supernatant was removed. At time 0, 0.5 mL of 50-nm silica NPs was added to the upper chamber at a concentration of 300 µg/mL and 1.5 mL of media was added to the lower chamber. After 2, 4, 6, 8, 12, 16, 20 and 24 h, a 50-µL aliquot of the medium was collected from the lower chamber, which was transferred to a 96-well opaque plate, and 50 µL of the medium was added to the lower chamber. After the last collection of the medium, the TEER was measured, and the cells were washed, as indicated above. The membranes were excised, fixed in 2% paraformaldehyde for 40 min, permeabilized in 0.3% Triton X-100 for 20 min at room temperature, and blocked in 3% BSA in PBS for 1 h at room temperature. The cells were incubated with the rabbit anti-human ZO-1 antibody (diluted 1:100 in 2% bovine serum albumin in PBS) for 18 h at 4°C, followed by the secondary antibody (diluted 1:1000 in PBS) for 1 h at room temperature in the dark. The nuclei were stained with DAPI, and the membranes were mounted on glass slides. The cells were observed under a confocal laser scanning microscope (A1R+; Nikon Ltd., Tokyo, Japan), and the images were processed with NIS-Elements Viewer 5.21 Software (Tokyo, Japan). To examine the effects of the inhibitors on the uptake of silica NPs, the cells were cultured on Transwell inserts and pre-incubated with silica NPs. The concentrations of the inhibitors were the same as those of previous experiments, and the percent uptake was calculated, as indicated above.

2.10 Statistical Analysis

The results were expressed as mean ± SD. Data were analyzed with SPSS 21.0 software version (SPSS Inc., Chicago, IL, USA) and GraphPad Prism 8.0.1 (Graph-Pad Software, Inc., San Diego, CA, USA), and one-way analysis of variance (ANOVA) was used for multi group comparison. Differences were considered statistically significant at P values less than 0.05.

3. Results

3.1 Characterization of Silica NPs

The silica NPs were uniform in size and spherical in shape (Fig. 1A-C). The diameters of the silica NPs were determined by SEM to be 36.0 ± 4.8 nm, 54.0 ± 6.0 nm, and 133.9 ± 19.4 nm (n = 100), and the distribution of the sizes was assessed by DLS to be narrow (Fig. 1D-F). The ζ potentials were -25.56 ± 1.354 mV, -37.36 ± 1.790, and -33.63 ± 2.661 (n = 3), which indicated they had good stability in aqueous solutions.

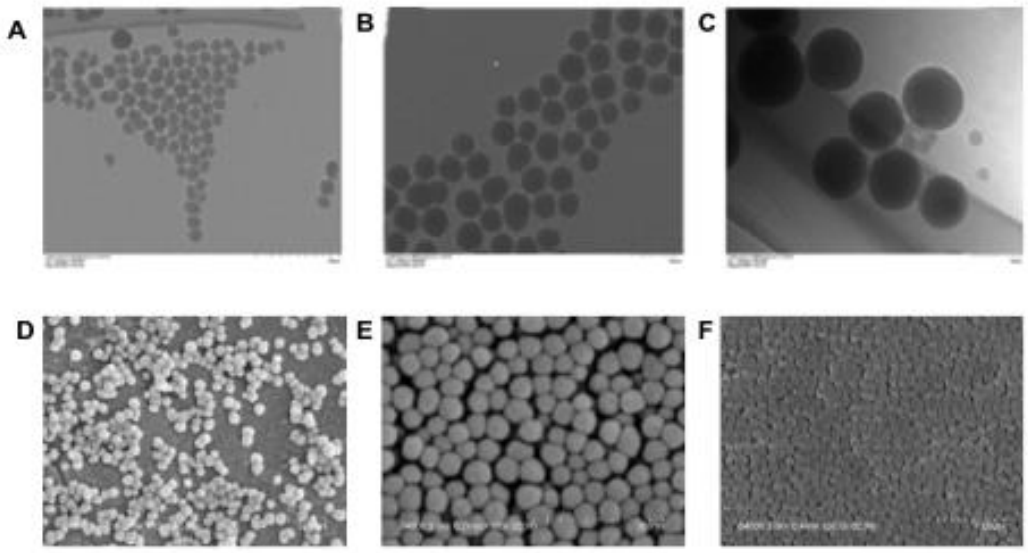

Figure 1: TEM images of silica NPs. (A) 20-nm silica NPs, (B) 50-nm silica NPs, and (C) 100-nm silica NPs. SEM images of silica NPs. (D) 20-nm silica NPs, (E) 50-nm silica NPs, and (F) 100-nm silica NPs.

3.2 CCK-8 Cytotoxicity Assay

Silica NPs at concentrations <400 µg /mL were not cytotoxic. However, 50-nm and 100-nm silica NPs at concentrations >400 µg/mL were cytotoxic, and 20-nm silica NPs at a concentration of 800 µg/mL were also cytotoxic (Fig. 2). Therefore, uptake and transport assays were performed at a concentration below of 300 µg/mL. Uptake of silica NPs of different sizes and concentrations.

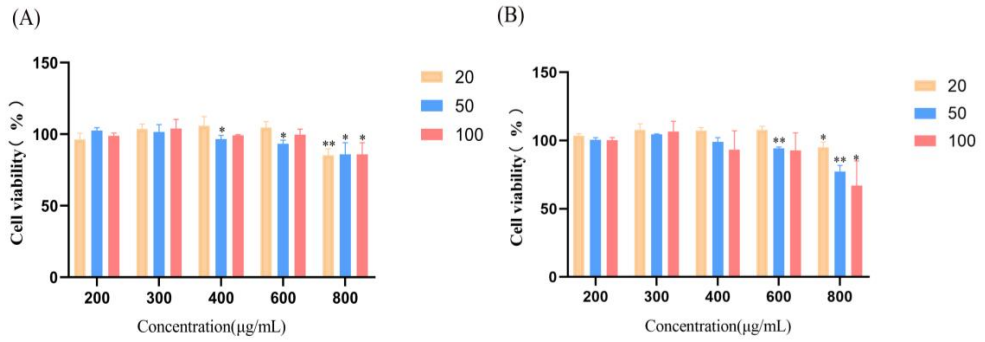

Figure 2: Viability of BeWo b30 Cells Exposed to Silica NPs for 24 and 48 h. Each Value was Represented the Mean ± SD (n = 5).

The uptake of silica NPs increased as the concentration of silica NPs elevated (Fig. 3), which manifested that the uptake by BeWo b30 cells was not saturated at 300 μg/mL. At concentrations of 75 and 150 μg/mL, the uptake of 50-nm silica NPs was significantly greater than that of 20-nm and 100-nm silica NPs. At a concentration of 300 μg/mL, the uptake of 100-nm silica NPs was the greatest, which demonstrated that the internalization of silica NPs was related to size.

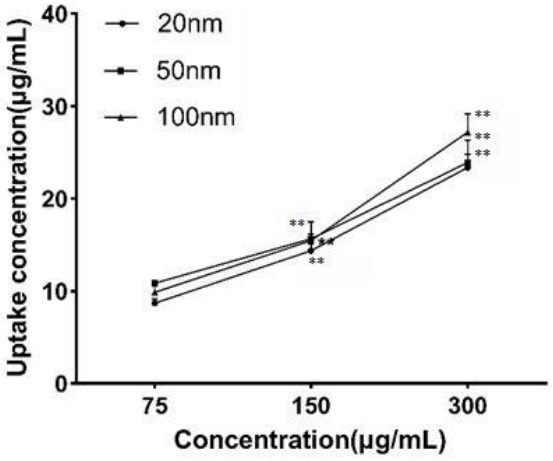

Figure 3: Dose-dependent uptake of silica NPs by BeWo b30 cells. The cells were incubated with 20-nm, 50-nm and 100-nm silica NPs (300 μg/mL) for 5 h, and the uptake was quantified by fluorometry. Data were represented as mean ±SD of five determinations. **P<0.01 compared to a concentration of 75 μg/mL.

3.3 Monolayer Confirmation

TEER values higher than 60 Ω cm^2 were considered acceptable for performing subsequent transport experiments [14]. On day 5, the results of TEER and Na-Flu assays confirmed the formation of the BeWo b30 cell monolayer (Fig. 4A). On day 6, the results of ZO-1 staining further confirmed the formation of the cell monolayer. The nuclei were visualized with DAPI (Fig. 4B).

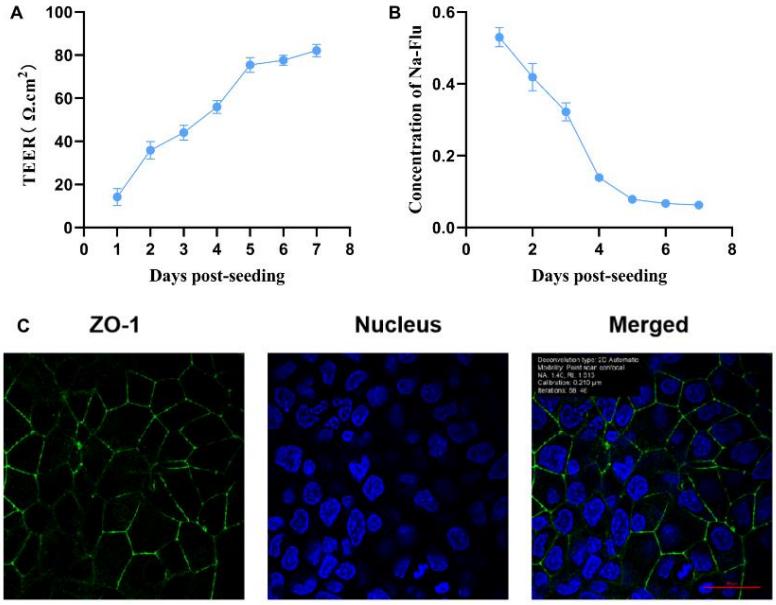

Figure 4: Formation of BeWo b30 Cell Monolayer. (A) Results of TEER assay, (B) Results of Na-Flu transport assay. Data were represented as mean ± SD of five determinations. Confocal images of BeWo b30 cells fluorescently stained for ZO-1. (C) The cells were cultured on Transwell units and stained with an antibody against ZO-1 (green). The cell nuclei were stained with DAPI (blue).

3.4 Transport of Silica NPs

The results of the transport of silica NPs across the BeWo b30 cell monolayer were shown in (Fig. 5). The rate of increase was rapid between 0 h and 12 h, with the amount of transport increasing from 20.42 μg/mL to 60.5 μg/mL. After 12 hours, the rate of increase began to flatten out, with a mere increase of 7.6 μg/mL observed between the 12th and 24th hour. These results indicated that silica NPs were capable of transplacental transport.

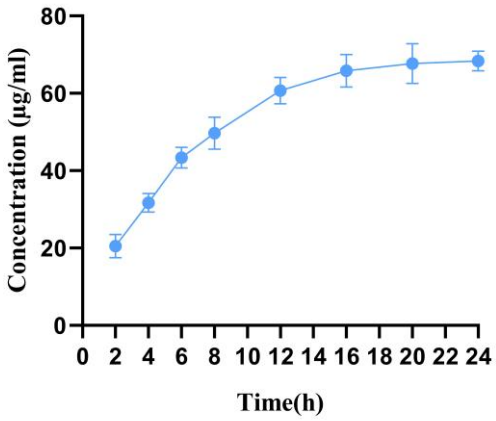

Figure 5: Transport of 50-nm silica NPs across the BeWo b30 cell monolayer. The cells were incubated with 50-nm silica NPs at a concentration of 300 μg/mL for 24 h, and the concentrations of silica NPs in the lower chamber were quantified at different time points by fluorometry. Data were represented as mean ± SD of three determinations.

3.5 Endocytic Mechanism of Silica NPs

The internalizations of 20-nm, 50-nm and 100-nm silica NPs were reduced dramatically after treating cells with inhibitors of endocytosis ($P<0.05$ or $P<0.01$) (Fig. 6A). CPZ manifested the most pronounced inhibitory effect, and the inhibition rates of 20-nm, 50-nm, and 100-nm silica NPs reached 57.5%, 49.6% and 46.9%, respectively. NY also indicated a remarkable inhibitory effect, and the inhibition rates of 20-nm, 50-nm, and 100-nm silica NPs touched 43.2%, 34.9% and 39.4%, respectively.

By confocal microscopy, silica NPs were observed in the cytoplasm of BeWo b30 cells (Fig. 6B). The number of silica NPs was reduced in CPZ- and NY-treated cells compared with Col- and AMR-treated cells, which indicated that the internalization of silica NPs involved clathrin- and caveolin-mediated endocytosis.

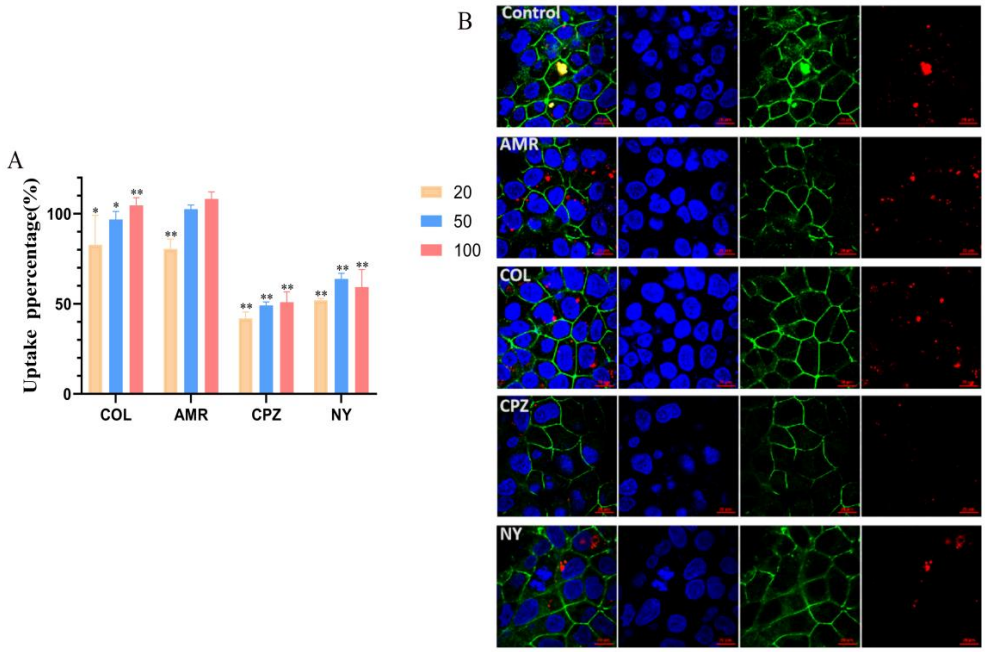

Figure 6: Effects of inhibitors of endocytosis on the internalization of silica NPs. BeWo b30 cells were pre-treated with different inhibitors of endocytosis for 1 h and then treated with silica NPs at a concentration of 300 µg/mL. The percent uptake was quantified by fluorometry. (A). Data were presented as mean ±SD of five determinations. *P<0.05, **P<0.01 compared to respective controls. AMR, amiloride; Col, colchicine; CPZ, chlorpromazine; NY, nystatin. Confocal images of BeWo b30 cells treated with different inhibitors of endocytosis. (B) The cells were cultured on Transwell units, treated with AMR, Col, CPZ or NY as indicated, and stained with an antibody against ZO-1 (green). The cell nuclei were stained with DAPI (blue). Silica NPs (diameter, 50-nm; red) were shown in the cytoplasm.

3.6 PI3K/AKT/GSK3β Signaling Pathway in the Endocytosis of Silica NPs

To investigate the dose-dependent effects of the PI3K/AKT inhibitor on the uptake of 50-nm silica NPs, BeWo b30 cells were pre-treated with LY294002 at concentrations of 2.5, 5 and 10 µM for 30 min. All three doses of the inhibitor affected the internalization of silica NPs dose-dependently, with inhibitory rates of 31.05%, 36.14% and 43.53%, respectively (P<0.01) (Fig. 7). The levels of PI3K, AKT, and GSK3β were evaluated by western blot. When the cells were treated with silica NPs, the levels of p-PI3K/PI3K, p-AKT/AKT and p-GSK3β/GSK3β increased compared with control cells. However, when the cells were pretreated with LY294002 and then treated with silica NPs, the levels of these proteins decreased (P<0.05 or P<0.01) (Fig. 8). By confocal microscopy, the number of silica NPs in the cytoplasm of cells treated with LY294002 decreased compared with control cells, especially at concentrations of 5 and 10 µM (Fig. 9). These findings were consistent with those of uptake assays, which indicated that the PI3K/AKT/GSK3β signaling pathway played important role in internalization of the silica NPs.

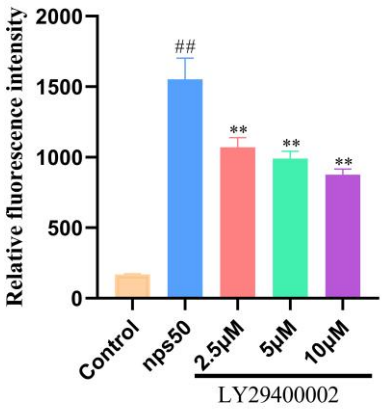

Figure 7: Effects of the PI3K/AKT inhibitor on the internalization of silica NPs. BeWo b30 cells were pre-treated with LY294002 for 30 min and then treated with 50-nm silica NPs at a concentration of 300 µg/mL. Internalization was quantified by fluorometry. Data were represented as mean ±SD of five determinations. *P<0.05, **P<0.01 compared to 50-nm silica NPs alone.

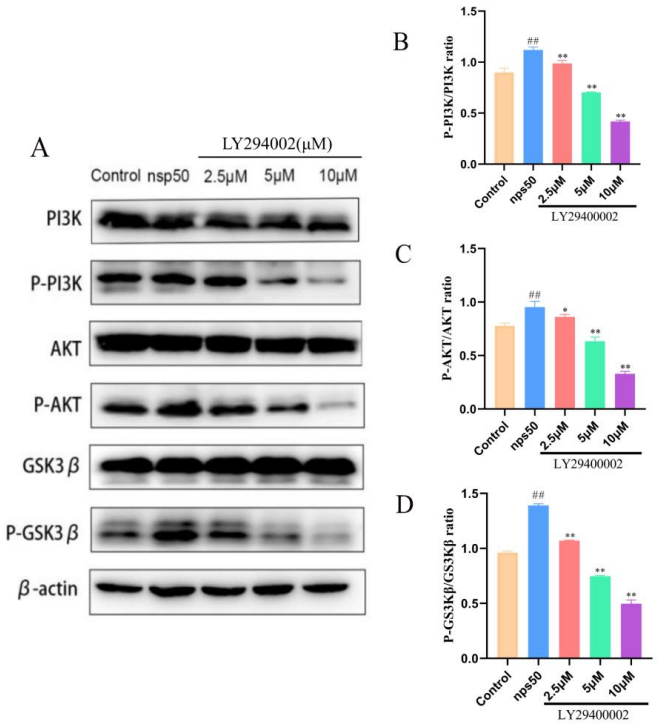

Figure 8: Levels of PI3K, P-PI3K, AKT, P-AKT, GSK3β, and P-GSK3β following treatment. BeWo b30 cells were pre-treated with LY294002 at different concentrations (2.5, 5, 10 μM) for 30 min and then treated with 100-nm silica NPs at a concentration of 300 μg/mL. Protein levels were quantified by western blotting. Data were represented as mean ± SD of three determinations. #P<0.05, ##P<0.01 compared to respective controls; *P<0.05, **P<0.01 compared to 50-nm silica NPs alone.

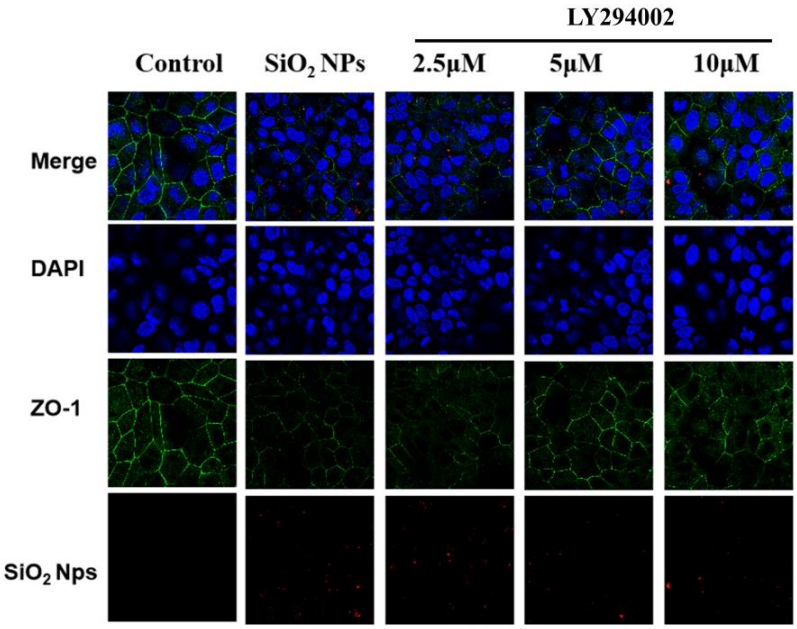

Figure 9: Confocal images of BeWo b30 cells treated with the PI3K/AKT inhibitor. BeWo b30 cells were treated with LY294002 at different concentrations (2.5, 5, 10 μM). The tight junction protein ZO-1 was stained, and the cell nuclei were stained with DAPI. Silica NPs (diameter, 100 nm; red) were shown in the cytoplasm.

4. Discussion

Only a few drugs have been approved for pregnancy-related disorders over the last two decades, and the efficacy of existing therapeutic agents is extremely limited [15]. Nanomedicine has created opportunities for novel modalities in the delivery of drugs in pregnant women, which increases the safety and efficacy of drugs due to their long half-life, slow and controlled release, and tissue specificity [16,8]. However, the fetal toxicity of nanomaterials is understudied. The aim of this study was to determine the transport mechanism of silica NPs through the placenta. In the experiment, there were no apparent toxic effects of silica NPs of different sizes on BeWo b30 cells,

consistent with the results of Correia and his colleagues [17]. At concentrations > 400 μg/mL, silica NPs of different sizes decreased the viability of cells. Therefore, the concentration of silica NPs used in uptake and transport assays was 300 μg/mL. The uptake of silica NPs at different concentrations was observed, with greater internalization of 50-nm silica NPs than 20-nm silica NPs. According to the results of previous studies NP internalization increases with NP size, and the uptake rate was highest for 45–50-nm NPs, whereas the exocytic rate was fastest for smaller NPs 17. Correia and his colleagues did not observe a relationship between NP size and transport rate, but this could be explained by the overlap in the size distribution of silica NPs [17].

BeWo b30 cells can establish a monolayer, and they are often used as a model of the human placental barrier for studying transplacental transport [27]. We evaluated the formation of the cell monolayer from days 1 to 7 using TEER and Na-Flu transport assays, and observed that tight junctions were established during this time. By day 5, TEER values reached the desirable range of a previous study, and Na-Flu transport was retardated, which indicated that cells could be used for subsequent experiments. By fluorescent staining, we observed tight junction formation on day 6, consistent with the results of previous studies [6,13,8]. Furthermore, we observed maximal internalization of 50-nm silica NPs at 12 h, followed by a plateau in the curve. Poulsen and his groups reported maximal internalization of 25-nm silica NPs after 12 h, followed by a slight decrease after 24 h [13].

The cellular uptake of NPs was suppressed by inhibitors of endocytosis. CPZ, a selective inhibitor of clathrin-mediated endocytosis, demonstrated the most pronounced effect, followed by the caveolin-mediated endocytosis inhibitor, NY, and these findings were confirmed by confocal microscopy. These results manifested that clathrin- and caveolae-mediated endocytosis were involved in the internalization of silica NPs, consistent with a previous study that revealed clathrin-mediated endocytosis of 310-nm silica NPs in HUVEC [28]. Another study in fibroblasts demonstrated that 500-nm silica NPs were internalized by clathrin-mediated endocytosis and macropinocytosis but 80-nm NPs were internalized by clathrin-mediated endocytosis, micropinocytosis, and caveolae-mediated endocytosis [19]. Taken together, clathrin- and caveolin-dependent mechanisms play roles in the uptake of silica NPs of different sizes.

Clathrin-mediated endocytosis involves the formation, stabilization, and maturation of clathrin-coated pits, and clathrin, dynamin, and adaptor protein 2 are the key proteins involved in this process [30]. There are three dynamin isoforms, Dyn1, Dyn2, and Dyn3. Dyn1 is widely expressed in non-neuronal cells and inactivated in non-neuronal cells through phosphorylation by GSK3β [23]. However, Reis and his fellow scientists reported that Dyn1 could be activated in non-neuronal cells and alter the rate of clathrin-mediated endocytosis, thereby link endocytosis to AKT/GSK3β signaling pathways [20]. The transferrin receptor (TfnR) is the specific receptor for transferrin, and it is internalized through a clathrin-dependent pathway [21]. In another study, GSK3β inhibitors could decrease Dyn1 phosphorylation and increase TfnR internalization, while PI3K/AKT inhibitors could activate GSK3β and decrease TfnR internalization in H1299 cells [22]. It was found that inhibition of GSK3β was ineffective in preventing TfnR internalization following Dyn1 knockdown, thereby indicated that GSK3β is influenced by Dyn1 [23]. Therefore, clathrin-mediated endocytosis was regulated by the PI3K/AKT/GSK3β signaling pathway. Here, LY294002 was used to inhibit PI3K/AKT, and we observed that the internalization of silica NPs was reduced dose-dependently. To illustrate the relationship between endocytosis and the related gene protein expressions of PI3K/AKT/GSK3β signaling pathway were examined by western blot. The levels of p-PI3K/PI3K, p-AKT/AKT, and p-GSK3β/GSK3β increased in cells treated with silica NPs. Interestingly, it has been reported that GSK3β phosphorylation could reduce its activity [24], which promoted Dyn1 phosphorylation and clathrin-mediated endocytosis. In the presence of LY294002, the phosphorylation levels of all proteins decreased dose-dependently, and was consistent with the results of Wang and his fellow scientists, who reported that treatment of bovine aortic endothelial cells with 70-nm silica NPs increased the p-AKT/AKT level compared with the control, whereas wortmannin, a selective PI3K inhibitor, lessened its expression level [26]. Therefore, the PI3K/AKT/GSK3β signaling pathway had important roles in the uptake and transport of silica NPs in BeWo b30 cells.

5. Conclusion

The present study authenticated for the first time that silica NPs could cross the BeWo b30 cell monolayer, and they were internalized by clathrin- and caveolin- mediated endocytosis, which was regulated by the PI3K/AKT/GSK3β signaling pathway (Fig. 10). The internalization of silica NPs by BeWo b30 cells was affected by the size of NPs. Our findings manifested that this approach of endocytic inhibition could reduce the fetal toxicity of nanomedicines and promote their application in perinatal medicine.

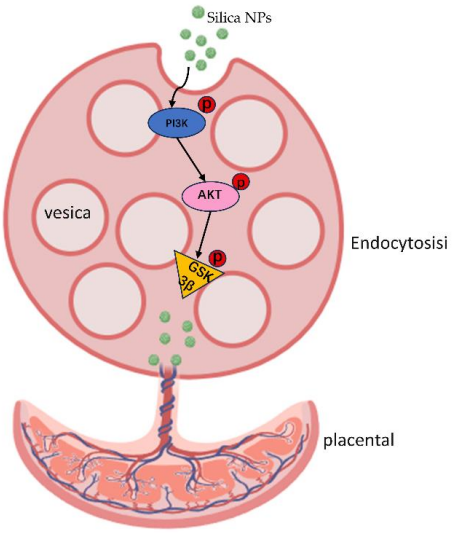

Figure 10: Silica NPs could penetrate the placental barrier model of BeWo b30 cells in vitro, entering mainly through clathrin and caveolin-mediated endocytosis regulated by the PI3K/Akt/GSK3β signaling pathway.

Declaration of Competing Interest

The authors declare that they have no competing interests.

Ethics Approval

The cells used in this experiment were not primary cells and were donated by Professor Erik Rytting (University of Texas Medical Branch).

Funding

This work was supported by the Key Projects of Traditional Chinese Medicine of Hubei Provincial Health Commission (No. ZY2023Z015); the Zhejiang Basic Public Welfare Research Program (No. LGF21H090002); the Zhejiang Medical and Health Science and Technology Plan Project (No. 2022497454); the Natural Science Foundation of Hubei science and Technology Department (No. 2022CFB357, 2022CFB427) and the Open Foundation of Capital Medical University (No. PYZ2018126, PYZ19056).

Author Contribution Statement

THB and WMY: conceived the ideas and conducted the experiments, analyzed the data, wrote the manuscript. HJY, XF and JWJ: performed the experiments, analyzed the data, provided critical materials. YCH, HHB and WHW conceived the ideas and designed the experiments, analyzed the data and revised the manuscript. All the authors have read and approved the final version for publication.

Acknowledgements

Thanks for Professor Erik Rytting (University of Texas Medical Branch) for donating the choriocarcinoma cell line BeWo b30 and all the participants and contributors.

References

1. Adepu, S., & Ramakrishna, S. (2021). Controlled drug delivery systems: current status and future directions. *Molecules, 26*(19), 5905.
2. Aengenheister, L., Favaro, R. R., Morales-Prieto, D. M., Furer, L. A., Gruber, M., Wadsack, C., ... & Buerki-Thurnherr, T. (2021). *Research on nanoparticles in human perfused placenta: State of the art and perspectives. Placenta, 104,* 199-207.
3. Farjadian, F., Ghasemi, A., Gohari, O., Roointan, A., Karimi, M., & Hamblin, M. R. (2019). Nanopharmaceuticals and nanomedicines currently on the market: challenges and opportunities. *Nanomedicine, 14*(1), 93-126.
4. Sato, Y., Nakamura, T., Yamada, Y., & Harashima, H. (2021). The nanomedicine rush: new strategies for unmet medical needs based on innovative nano DDS. *Journal of controlled release, 330,* 305-316.
5. Cooke, L. D., Tumbarello, D. A., Harvey, N. C., Sethi, J. K., Lewis, R. M., & Cleal, J. K. (2021). Endocytosis in the placenta: An undervalued mediator of placental transfer. *Placenta, 113,* 67-73.
6. Albekairi, N. A., Al-Enazy, S., Ali, S., & Rytting, E. (2015). Transport of digoxin-loaded polymeric nanoparticles across BeWo cells, an in vitro model of human placental trophoblast. *Therapeutic Delivery, 6*(12), 1325-1334.
7. Kloet, S. K., Walczak, A. P., Louisse, J., van den Berg, H. H., Bouwmeester, H., Tromp, P., ... & Rietjens, I. M. (2015). Translocation of positively and negatively charged polystyrene nanoparticles in an in vitro placental model. *Toxicology in Vitro, 29*(7), 1701-1710.
8. Tang, H., Jiang, Z., He, H., Li, X., Hu, H., Zhang, N., ... & Zhou, Z. (2018). Uptake and transport of pullulan acetate nanoparticles in the BeWo b30 placental barrier cell model. *International Journal of Nanomedicine*, 4073-4082.
9. Yang, Y., Zhang, M., Song, H., & Yu, C. (2020). Silica-based nanoparticles for biomedical applications: from nanocarriers to biomodulators. *Accounts of chemical research, 53*(8), 1545-1556.
10. Yamashita, K., Yoshioka, Y., Higashisaka, K., Mimura, K., Morishita, Y., Nozaki, M., ... & Tsutsumi, Y. (2011). Silica and titanium dioxide nanoparticles cause pregnancy

complications in mice. *Nature nanotechnology, 6*(5), 321-328.
11. Carter, A. M. (2020). Animal models of human pregnancy and placentation: alternatives to the mouse. *Reproduction, 160*(6), R129-R143.
12. Poulsen, M. S., Mose, T., Maroun, L. L., Mathiesen, L., Knudsen, L. E., & Rytting, E. (2015). Kinetics of silica nanoparticles in the human placenta. *Nanotoxicology, 9*(sup1), 79-86.
13. Cartwright, L., Poulsen, M. S., Nielsen, H. M., Pojana, G., Knudsen, L. E., Saunders, M., & Rytting, E. (2012). In vitro placental model optimization for nanoparticle transport studies. *International journal of nanomedicine,* 497-510.
14. Mørck, T. J., Sorda, G., Bechi, N., Rasmussen, B. S., Nielsen, J. B., Ietta, F., ... & Knudsen, L. E. (2010). Placental transport and in vitro effects of Bisphenol A. *Reproductive toxicology, 30*(1), 131-137.
15. Pereira, K. V., Giacomeli, R., de Gomes, M. G., & Haas, S. E. (2020). The challenge of using nanotherapy during pregnancy: Technological aspects and biomedical implications. *Placenta, 100*, 75-80.
16. Figueroa-Espada, C. G., Hofbauer, S., Mitchell, M. J., & Riley, R. S. (2020). Exploiting the placenta for nanoparticle-mediated drug delivery during pregnancy. *Advanced Drug Delivery Reviews, 160*, 244-261.
17. Correia Carreira, S., Walker, L., Paul, K., & Saunders, M. (2015). The toxicity, transport and uptake of nanoparticles in the in vitro BeWo b30 placental cell barrier model used within NanoTEST. *Nanotoxicology, 9*(sup1), 66-78.
18. Nam, J., Won, N., Bang, J., Jin, H., Park, J., Jung, S., ... & Kim, S. (2013). Surface engineering of inorganic nanoparticles for imaging and therapy. *Advanced drug delivery reviews, 65*(5), 622-648.
19. Soenen, S. J., Manshian, B., Doak, S. H., De Smedt, S. C., & Braeckmans, K. (2013). Fluorescent non-porous silica nanoparticles for long-term cell monitoring: cytotoxicity and particle functionality. *Acta biomaterialia, 9*(11), 9183-9193.
20. Reis, C. R., Chen, P. H., Bendris, N., & Schmid, S. L. (2017). TRAIL-death receptor endocytosis and apoptosis are selectively regulated by dynamin-1 activation. *Proceedings of the National Academy of Sciences, 114*(3), 504-509.
21. Gammella, E., Buratti, P., Cairo, G., & Recalcati, S. (2017). The transferrin receptor: the cellular iron gate. *Metallomics, 9*(10), 1367-1375.
22. Reis, C. R., Chen, P. H., Srinivasan, S., Aguet, F., Mettlen, M., & Schmid, S. L. (2015). Crosstalk between Akt/GSK 3β signaling and dynamin-1 regulates clathrin-mediated endocytosis. *The EMBO journal, 34*(16), 2132-2146.
23. Srinivasan, S., Burckhardt, C. J., Bhave, M., Chen, Z., Chen, P. H., Wang, X., ... & Schmid, S. L. (2018). A noncanonical role for dynamin-1 in regulating early stages of clathrin-mediated endocytosis in non-neuronal cells. *PLoS biology, 16*(4), e2005377.
24. Eiraku, N., Chiba, N., Nakamura, T., Amir, M. S., Seong, C. H., Ohnishi, T., ... & Matsuguchi, T. (2019). BMP9 directly induces rapid GSK3-β phosphorylation in a Wnt-independent manner through class I PI3K-Akt axis in osteoblasts. *The FASEB Journal, 33*(11), 12124.
25. Wang, Y., Wei, Z., Xu, K., Wang, X., Gao, X., Han, Q., ... & Chen, M. (2023). The effect and a mechanistic evaluation of polystyrene nanoplastics on a mouse model of type 2 diabetes. *Food and Chemical Toxicology, 173,* 113642.
26. Onodera, A., Yayama, K., Tanaka, A., Morosawa, H., Furuta, T., Takeda, N., ... & Kawai, Y. (2016). Amorphous nanosilica particles evoke vascular relaxation through PI 3K/Akt/eNOS signaling. *Fundamental & Clinical Pharmacology, 30*(5), 419-428.
27. Abdelkhaliq, A., van der Zande, M., Peters, R. J., & Bouwmeester, H. (2020). Combination of the BeWo b30 placental transport model and the embryonic stem cell test to assess the potential developmental toxicity of silver nanoparticles. *Particle and Fibre Toxicology, 17*, 1-16.
28. Blechinger, J., Bauer, A. T., Torrano, A. A., Gorzelanny, C., Bräuchle, C., & Schneider, S. W. (2013). Uptake kinetics and nanotoxicity of silica nanoparticles are cell type dependent. *Small, 9*(23), 3970-3980.
29. Li, H., van Ravenzwaay, B., Rietjens, I. M., & Louisse, J. (2013). Assessment of an in vitro transport model using BeWo b30 cells to predict placental transfer of compounds. *Archives of toxicology, 87,* 1661-1669.
30. Wang, X., Qiu, Y., Wang, M., Zhang, C., Zhang, T., Zhou, H., ... & Shao, R. (2020). Endocytosis and organelle targeting of nanomedicines in cancer therapy. *International journal of nanomedicine,* 9447-9467.